Journal of Hazardous Materials 366 (2019) 329–337

Contents lists available at ScienceDirect

Journal of Hazardous Materials

journal homepage: www.elsevier.com/locate/jhazmat

Benzo(a)pyrene degradation by cytochrome P450 hydroxylase and the functional metabolism network of *Bacillus thuringiensis*

Qiying Lu[a], Kaiyun Chen[b], Yan Long[c], Xujun Liang[c], Baoyan He[c], Lehuan Yu[a], Jinshao Ye[c,*]

[a] College of Biology and Food Engineering, Guangdong University of Education, Guangzhou, 510303, Guangdong, China
[b] Child Developmental-Behavioral Center, The Third Affiliated Hospital of Sun Yat-sen University, Guangzhou, 510630, China
[c] Guangdong Key Laboratory of Environmental Pollution and Health, School of Environment, Jinan University, Guangzhou, 510632, China

ARTICLE INFO

Keywords:
Biosorption
Metabonomics
Benzo(a)pyrene
Phospholipid
Metabolism pathway

ABSTRACT

The relationship between benzo(a)pyrene biodegradation and certain target biomolecules has been investigated. To regulate the degradation process, the associated metabolism network must be clarified. To this end, benzo(a) pyrene degradation, carbon substrate metabolism and exometabolomic mechanism of *Bacillus thuringiensis* were analyzed. Benzo(a)pyrene was degraded through hydroxylation catalyzed by cytochrome P450 hydroxylase. After the treatment of 0.5 mg L^{-1} of benzo(a)pyrene by 0.2 g L^{-1} of cells for 9 d, biosorption and degradation efficiencies were measured at approximately 90% and 80%, respectively. During this process, phospholipid synthesis, glycogen, asparagine, arginine, itaconate and xylose metabolism were significantly downregulated, while glycolysis, pentose phosphate pathway, citrate cycle, amino sugar and nucleotide sugar metabolism were significantly upregulated. These findings offer insight into the biotransformation regulation of polycyclic aromatic hydrocarbons.

1. Introduction

Polycyclic aromatic hydrocarbons (PAHs) are a class of ubiquitous organic contaminants characterized by the presence of at least two fused aromatic rings. PAHs are widely distributed in the environment through various processes such as the production and combustion of organic materials from anthropogenic and natural activities [1]. Although the joint effects of chemical oxidation, photolysis and volatilization contribute to PAH removal [2], the low solubility and bioavailability of PAHs results in their accumulation in ecosystems and organisms. Biodegradation is an environmentally sustainable measure for the elimination of PAHs from terrestrial and aquatic environments [3–5]. Some effective microbes have been selected for the degradation or cometabolic oxidization of high molecular weight PAHs (Table S1).

With cytotoxic, mutagenic, carcinogenic and accumulative properties, benzo(a)pyrene (BaP) is a model compound for the investigation of metabolic information related to PAH biodegradation [6,7]. Based on BaP identified intermediates such as BaP-7,8-diol-9,10-epoxide, BaP-1,6-quinone, 1-hydroxy-2-benzoic acid and benzoic acid, the cleavage pathway of benzene rings has been identified [8–10]. During cleavage, the expression of cytochrome P450 s has been induced [8,9] for the biotransformation of BaP through the aryl hydrocarbon receptor pathway [11]. A member of this protein family, cytochrome P4501 A, expressed in an engineered *Shewanella oneidensis* has been verified to be an enzyme of catalyzed BaP [12].

The synthesis of heat shock proteins, arginine kinase, glutathione S-transferases, UDP-glucuronosyltransferases and sulfotransferases has been enhanced to relieve stress from BaP and its intermediates through conjugation reactions [13–15]. Among these proteins, heat shock proteins have been synthesized in response to exposure to stress while glutathione S-transferases catalyze the conjugation of the reduced form of glutathione to xenobiotic substrates for detoxification. S-layer proteins, ABC transporters and cysteine synthase with upregulated expression related to BaP transport by *Stenotrophomonas maltophilia* [16] and 22 genes in *Altererythrobacter epoxidivorans* associated with BaP degradation [17] have also been found. These findings offer insight into the relationship between BaP biodegradation and certain individual biomolecules. To regulate BaP degradation, metabolism networks associated with degradation must be identified. Metabolites are the end products of cellular processes catalyzed by functional proteins. The generation of metabolites and the transformation of nutrients during BaP degradation provide a direct functional readout of the metabolic states of functional microbes. Therefore, the functional metabolism network for the regulation of BaP degradation can be identified by investigating metabolites, including carbohydrates, organic acids, and phospholipids.

* Corresponding author.
E-mail address: folaye@126.com (J. Ye).

https://doi.org/10.1016/j.jhazmat.2018.12.004
Received 17 July 2018; Received in revised form 21 October 2018; Accepted 1 December 2018
Available online 03 December 2018
0304-3894/

Bacillus thuringiensis is a functional strain with crystal proteins that are highly toxic to susceptible insects. Its functional enzymes like cytochrome P450 s can effectively catalyze the cleavage of benzene rings, resulting in the degradation of triphenyltin [18], fipronil [19] and dimethyl phthalate [20]. It was used as a model strain to degrade BaP to identify interactions of BaP biodegradation and cellular metabolic networks in the present study. BaP degradation, substrate metabolisms and exometabolomic mechanisms were analyzed. Our findings offer insight into the metabolic regulation of PAH biotransformation.

2. Materials and methods

2.1. Microbe and chemicals

Samples of *B. thuringiensis* GIMCC1.817, an effective microbe for pollutant degradation [18], are stored in our lab and at the Microbiology Culture Center of Guangdong Province, China. BaP was purchased from Sigma–Aldrich (St. Louis, MO, USA). Culture medium contained (in g L^{-1}) 5 beef extract, 5 NaCl, 5 peptone and 0.05 $MgSO_4$. The M9 medium used for BaP degradation contained (in g L^{-1}) 12.8 $Na_2HPO_4{\cdot}7H_2O$, 3 KH_2PO_4, 0.5 NaCl, 1 NH_4Cl, 0.4 glucose, 0.24 $MgSO_4$, 0.01 $CaCl_2$, Wolfe's vitamin mixture and Wolfe's trace mineral mixture. A mixture of retention time markers for exometabolite analysis was prepared by dissolving fatty acid methyl esters (FAMEs) in chloroform. C8, C9, C10, C12, C14 and C16 concentrations of FAMES were measured as 0.8 g L^{-1} while C18, C20, C22, C24, C26, C28 and C30 levels were set to 0.4 g L^{-1}. A FAME mixture of 20 μL was added to 1 mL of *N*-methyl-*N*-trimethylsilytrifluoroacetamide (MSTFA) containing 1% trimethylchlorosilane to prepare a FAMEs/MSTFA mixture for exometabolite determination.

2.2. Benzo(a)pyrene biosorption and degradation

B. thuringiensis was inoculated into the culture medium at 30 °C in a rotary shaker at a rotation speed of 120 r min^{-1} for 24 h. Cells used for BaP degradation were separated from the medium by centrifugation at 6000 r min^{-1} for 5 min and then were rinsed three times with sterile M9 medium. Cells were inoculated at 100 r min^{-1} in flasks with 20 mL of M9 medium containing 0.5 mg L^{-1} of BaP in the dark at 25 °C on a rotary shaker. Effects of culturing time, pH values, degradation time and biomass dosages on BaP biosorption and degradation were assessed. In the experiments, culturing periods of 0.5 to 6 d, pH was set at 5.0, 5.5, 6.0, 6.5, 7.0, 7.5, 8.0, 8.5 and 9.0, and degradation periods ranged from 1 to 10 d. Biomass dosages were set to 0.01 to 0.50 g L^{-1}. After degradation, cells were separated by centrifugation at 6000 r min^{-1} for 5 min. Residual BaP in resultant supernatant was detected to determine removal efficiencies while residual BaP in the cells and supernatant was used to determine degradation efficiencies. To reveal the metabolism-independent process of BaP removal, *B. thuringiensis* at 0.01 to 0.5 g L^{-1} was inactivated by 2.5% glutaraldehyde for 24 h. These inactivated cells were then used to absorb BaP for 9 d. After separation, the supernatant was analyzed to determine adsorption efficiencies.

2.3. Extraction and measurement of benzo(a)pyrene

After degradation, residual BaP in the samples was extracted using a published method and was measured by gas chromatography-mass spectrometry (GC–MS, QP2010, Shimadzu) using an Rxi-5MS GC column (30 m × 0.25 mm × 0.25 μm) [21].

2.4. Carbon substrate metabolism for benzo(a)pyrene degradation

Biolog microplates were used to analyze the metabolism of extracellular carbon substrates. In brief, before and after BaP degradation cells were diluted in 0.85% sterilized saline solution 100 times followed by the inoculation of 150 μL of the mixture into each well of microplates at 25 °C in the dark. The optical density at 590 nm of each well was determined every 24 h. The metabolism network was mapped using the KEGG database (http://www.kegg.jp/).

2.5. Phospholipid extraction and analysis

After 7 d of BaP degradation, cells were extracted with 4 mL of Bligh-Dyer extractant in a horizontal shaker for 2 h at 25 °C. After centrifugation at 2500 r min^{-1} for 10 min, the supernatant was transferred to a clean glass centrifuge tube. Then, 1 mL of chloroform and 1 mL of water were added to the tube. The mixture was vortexed for 5 s and centrifuged for 10 min. After the removal of the upper liquid layer, the lower layer was evaporated at 30 °C in a speedvac. The extracted residue was dissolved in 1 mL of chloroform and transferred to a solid phase extraction cartridge. One milliliter of chloroform and 1 mL of acetone were used to wash the cartridge. The test tubes were placed in a vacuum manifold to remove solvents. Phospholipids in the tube were eluted with a 0.5 mL mixture of methanol: chloroform: H_2O (5:5:1) into a 1.5 mL glass vial, which was incubated at 37 °C for 15 min after 0.2 mL of transesterification reagent was added. The, 4.5 g L^{-1} of acetic acid and 0.4 mL of chloroform were added to each vial. The bottom layer at 0.3 mL was transferred to a vial with 4.5 g L^{-1} of acetic acid and 0.4 mL of chloroform. After phase separation, 0.4 mL of the bottom layer was transferred to a vial and then dried at room temperature. Hexane at 75 μL was used to dissolve the dried sample for GC–MS analysis. Before BaP degradation the control cells were prepared following the above procedure.

Phospholipids were measured using a GC–MS equipped with a DB-5MS (30 m × 0.25 mm × 0.25 μm) quartz capillary column. The conditions of GC–MS analysis were as follows: the column temperature was set to 140 °C for 2 min and then increased to 260 °C at a rate of 3 °C min^{-1}. He was used as a carrier gas. The sample inlet and ion source temperatures were set to 250 °C and 230 °C, respectively. The mass spectrometry scanning range was set to 50–500 m z^{-1}. Phospholipids were measured using peak areas.

2.6. Exometabolite analysis

An exometabolite analysis was performed according to [22]. Before and after degradation, cells were separated at 14,000 r min^{-1}. The samples without inoculation were used as control groups. One hundred microliters of supernatant were transferred to a centrifuge tube followed by the addition of 10 μL of labeled internal standard mixture (0.025 mM of ^{13}C cellobiose with 0.05 mM of ^{13}C glucose and ^{13}C xylose with ^{13}C vanillic acid, respectively). After lyophilization, 10 μL of methoxyamine hydrochloride solution was added to each tube and shaken at 1400 r min^{-1} at 30 °C for 1.5 h using an Eppendorf thermomixer. Then, 90 μL of FAMEs/MSTFA mixture was added to each tube and shaken at 1400 r min^{-1} at 37 °C for 30 min. After separation at 10,000 r min^{-1}, the supernatant was used for exometabolite analysis with an Agilent 7890 GC connected to an Agilent 5977 MS. Extraction blanks were prepared following the above procedure but starting with empty tubes.

Each sample of 2 μL was injected into the 50 °C injector port, which was ramped to 270 °C at a rate of 12 °C s^{-1} and held for 3 min. The GC was fitted with a 30 m long 0.25 mm ID Rtx5Sil-MS column. The initial oven temperature was set to 50 °C and increased by 5 °C min^{-1} to 65 °C and held for 0.2 min, was then increased by 15 °C min^{-1} to 80 °C and held for 0.2 min and was finally increased by 15 °C min^{-1} to 310 °C and held for 12 min. MS transfer line and ion source temperatures were set to 250 °C and 230 °C, respectively. Electron ionization was applied at 70 eV and mass spectra were acquired from 50 to 700 *m/z* at 8 spectra per second.

For data analysis FAMEs were used to measure the retention time. Raw data were deconvoluted into individual chemical peaks via Agilent MassHunter Unknowns Analysis software v.B.07.00 for Molecular

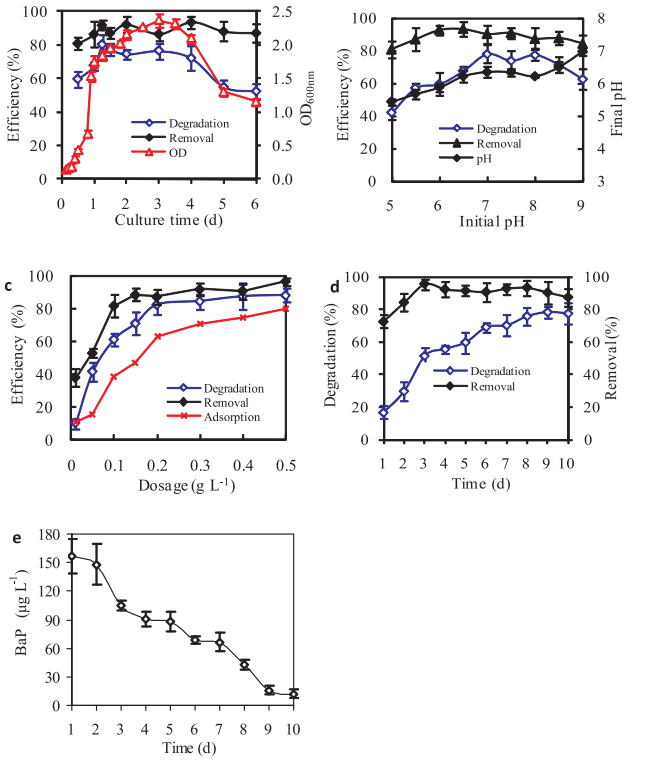

Fig. 1. Degradation of 0.5 mg L^{-1} of BaP at 25 °C by *Bacillus thuringiensis* (a) BaP degradation for 9 d by 0.2 g L^{-1} of cells separated from medium cultured for 0.5 to 6 d; (b) BaP degradation at pH 5 to 9 for 9 d by 0.2 g L^{-1} of cells; (c) BaP degradation for 9 d by 0.01 to 0.5 g L^{-1} of cells; (d) BaP degradation for 1 to 10 d by 0.2 g L^{-1} of cells; (e) Intracellular concentrations of BaP.

Feature Extraction. Compounds were identified by comparing the mass spectra and retention times of all deconvoluted peaks with an Agilent Fiehn Metabolomics Library (2013 version) containing the spectra profile. A mass spectral match factor of 75 or greater was determined a putative hit. Data alignment and quality control were performed using Mass Profiler Professional software. The list of metabolites was further then curated by comparing putatively identified metabolites to reference standards and by cross-checking mass spectra with the NIST metabolite database.

3. Results and discussion

3.1. Benzo(a)pyrene biosorption and degradation

Cells cultured for different periods of time were used to degrade BaP for 9 d (Fig. 1a). BaP degradation with an optimal efficiency level of approximately 80% by cells cultured for 30 h exhibited similar trends to the culture curve. According to data shown in Table S1, the degradation efficiencies of other PAHs such as phenanthrene and anthracene by certain strains reached up to 90%. These results show that the high molecular weight of PAHs is difficult to degrade. Cell separation at the stable phase with vigorous cellular activity resulted in high levels of degradation efficiency. Those in the apoptosis phase with limited capacity in terms of BaP-tolerance induced a decline in degradation efficiency.

After degradation, cells were separated by centrifugation at 6000 r min^{-1} for 5 min. BaP removal was identified when we observed in decline in BaP in the resultant supernatant, meaning that removal behavior involved surface adsorption, intracellular accumulation and metabolic degradation. Fig. 1a shows that BaP removal did not significantly correlate with cellular culture periods because removal primarily depended on levels of metabolism-independent adsorption. The lipid solubility of BaP triggered its adsorption because cellular membrane phospholipids tend to bind organic pollutants due to their hydrophobicity. BaP removal was more efficient than degradation throughout the process and especially at 0.5 and 6 d. These results confirm that some BaP accumulated within the cells. While *Selenastrum capricornutum* and *Scenedesmus acutus* also accumulated BaP, biodegradation was identified as the principal means of BaP removal [23]. Taking BaP removal, degradation levels and culture periods into account, cells cultured for 2 d were used in the following experiments.

The impact of pH values on BaP degradation was more significant than effects on removal levels (Fig. 1b). When initial pH values ranged from 5 to 9, removal efficiencies were maintained at above 80%, and the final pH values of each sample trended toward neutral values. This occurred because excessive H^+ and OH^- in the solutions reacted with cells, preventing the adsorption of BaP at the cellular surface. Moreover, BaP and its derivatives are membrane poisons. Joint exposure to BaP and excessive H^+/OH^- had detrimental effects on the membranes. Similar effects on the morphologies of cell walls and membranes of *B. thuringiensis* triggered by phenyltins have also been found [24].

BaP removal proved more efficient than degradation (Fig. 1), confirming that some BaP was absorbed by the cellular surface and accumulated in cytoplasm. Regarding degradation, a trend of increased efficiency was observed with pH values increasing from 5 to 7. Subsequently, a downward trend was observed. The suppression of BaP degradation in acidic and alkaline solutions primarily occurred due to effects of excessive H^+ and OH^- levels on the synthesis of proteome, which further prevented BaP binding and transformation. Proteomic regulation induced by tetracycline in solution at different pH values serves as direct evidence of the above inference [25]. Approximately one hundred proteins involved in ribosomes, bacterial chemotaxis, carbon metabolism, dicarboxylate metabolism, fatty acid biosynthesis, secondary metabolite biosynthesis, antibiotics biosynthesis, glycine, serine and threonine metabolism were downregulated in acidic and alkaline solutions [26]. Their downsynthesis finally inhibited pollutant resistance and transformation.

When the biomass dosage exceeded 0.2 g L^{-1}, the increased efficiencies of BaP removal and degradation tended to remain stable (Fig. 1c). This finding is partially attributed to limited contact between a single cell and BaP molecules. More nutrients were also needed to maintain cellular activity while biomass dosages were high, which accordingly depressed BaP treatment potential by a unit of biomass. This inference is supported by the metabolism of carbon substrates observed during BaP degradation (Fig. 3 and Table S2).

To illustrate the contributions of metabolism-independent processes to BaP removal, the adsorption capacity of BaP by inactivated cells of *B. thuringiensis* was investigated. Fig. 1c confirms that BaP can be removed from solution through metabolically independent activities. The above findings show that *B. thuringiensis* attracted and bound BaP by metabolism-independent adsorption, subsequently transporting it across cell membranes due to the metabolism or hydrophobicity of BaP and degrading it intracellularly.

To quantitatively measure the dynamic accumulation of BaP, residual BaP in solution and within cells was measured. Fig. 1d shows that the efficiency of BaP removal increased quickly and reached an optimal value over 3 d. Subsequently, it decreased to some extent followed by the equilibrium distribution of BaP between *B. thuringiensis* and the solution. In addition to resulting from effects of degradation, the accelerated removal process also partially resulted from physicochemical interactions between BaP and cellular surfaces occurring independent of cellular metabolic activities. The following equilibrium phase was related to biological metabolism, through which intracellular BaP could be released to the solution actively or leaked through the apoptosis of certain cells under BaP exposure over an extended contact period. The fact that BaP removal declined to same extent after 4 to 10 d of treatment serves as evidence of the occurrence of BaP release and leakage.

From the contrast observed between curves of removal and

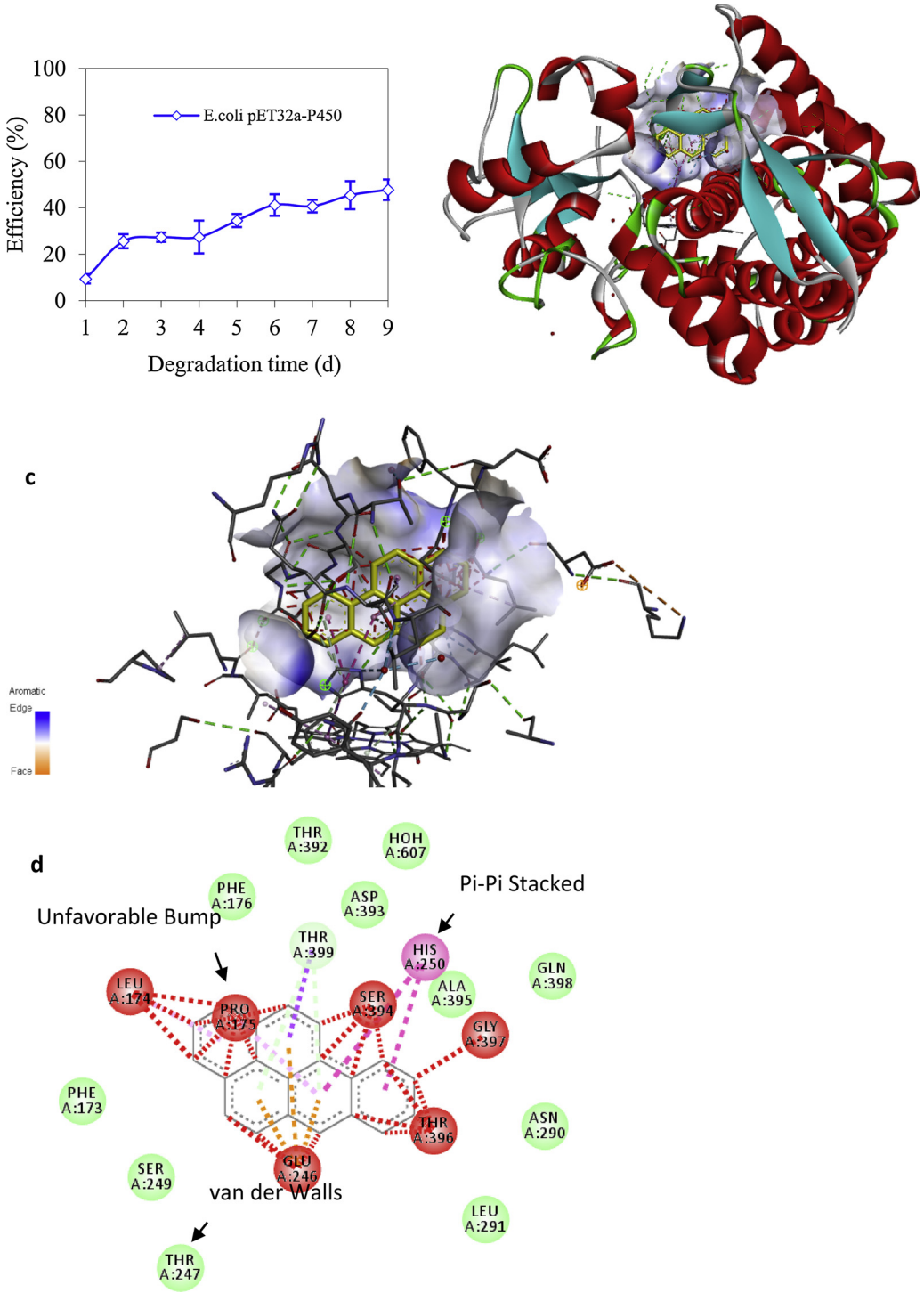

Fig. 2. (a) Degradation of 0.5 mg L^{-1} of BaP by 1 g L^{-1} of *Escherichia coli* pET32a-CYP450; (b) Interaction between P450 and BaP; (c) Active site for BaP binding; (d) Types of interaction between amino acids of active site and BaP.

degradation it can be deduced that large volumes of BaP accumulated in cells in the initial interval. With contact time, accumulated BaP slowly degraded. To understand this process, intracellular BaP was identified. The accumulation of intracellular BaP early on (Fig. 1e) shows that BaP can be quickly transported into a cell. In this period, some BaP was adsorbed into the cellular surface. With more exposure time, a decline in intracellular BaP shows that BaP degradation occurred intracellularly. These results further illustrate trends of BaP degradation observed throughout the degradation period. High concentrations of intracellular BaP observed early on enhanced contact between this component of BaP and cells, accordingly accelerating degradation while the later decline of intracellular BaP 3 d induced a decline in degradation kinetics.

3.2. Benzo(a)pyrene degradation by cytochrome P450 hydroxylase

To determine whether cytochrome P450 hydroxylase (P450) expressed in *B. thuringiensis* served as the enzyme for BaP degradation, *Escherichia coli* strain pET32a-P450 was used to degrade BaP. P450 with 404 amino acid residues expressed in *E. coli* pET32a-P450 was cloned

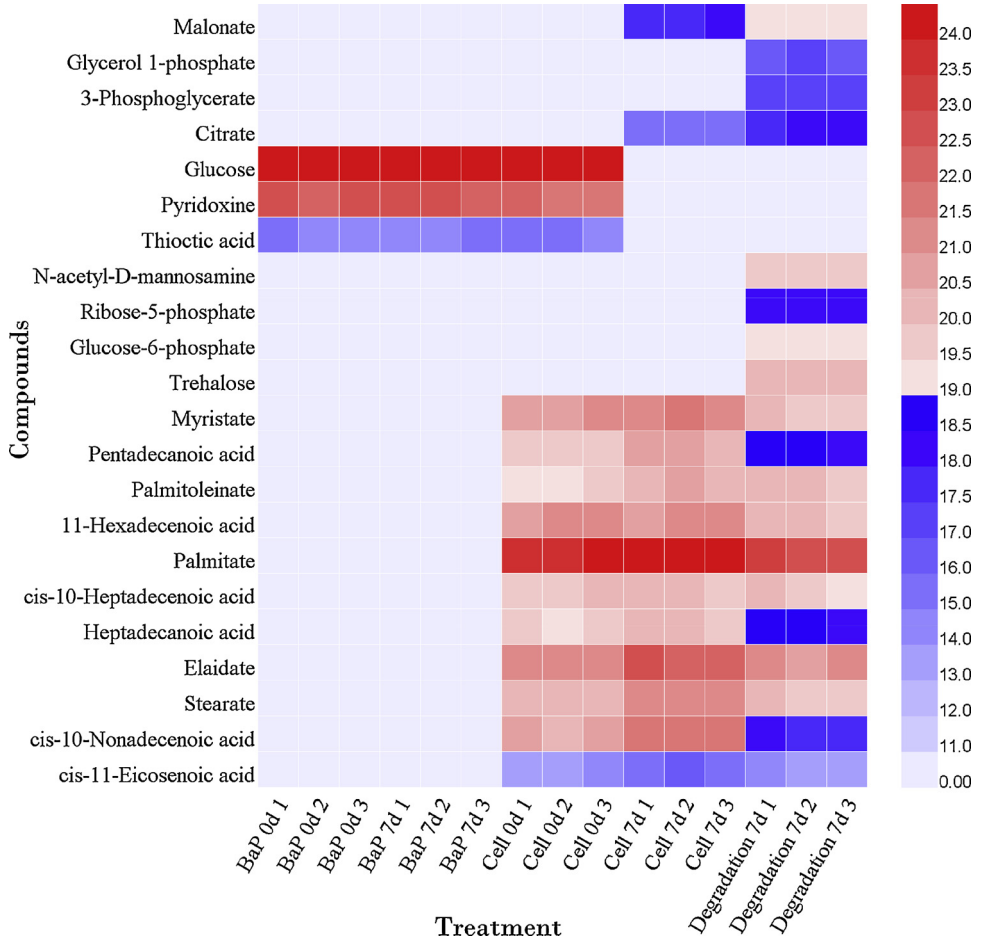

Fig. 3. Concentrations of exometabolites and phospholipids before or after BaP degradation for 7 d.

from *B. thuringiensis* [27]. The results show that this strain can degrade BaP while control cells of *E. coli* pET32a without P450 do not catalyze BaP (Fig. 2a). This finding confirms that P450 enzymes degrade BaP.

To identify potential substrate-binding residues, BaP molecule docking was performed using Discovery Studio software (version 2017R2). A structural comparison to other P450 s found in the PDB database (http://www.rcsb.org/) shows that the structure of the P450 studied in the current experiments is similar to the CYP106A2 (PDB: 5xnt) expressed in *Bacillus* sp. PAMC 23377 [28]. Therefore, the conformation of CYP106A2 likely reflected the functionally conformational state of the P450 studied in the current experiments and was used for substrate docking calculations. Before transformation, BaP was attracted by the pocket in P450 (Fig. 2b and c). The binding domain contained amino acids Leu^{174}, Pro^{175}, Glu^{246}, Ser^{394}, Thr^{396} and Gly^{397}, which adsorbed BaP through the unfavorable bump. Residue His^{250} bounded BaP through Pi-Pi interactions. $Phe^{173, 176}$, $Thr^{247, 392}$, Asn^{290}, Leu^{291}, Asp^{393}, Ala^{395}, Gln^{398}, Thr^{399} and Hoh^{607} attracted BaP via van der Walls (Fig. 2d). Then, BaP received an electron from ubiquinone oxidoreductase [27]. Oxygen was then bound and split into atoms through the attack of protons from ubiquinone oxidoreductase, forming the reactive species of P450 [29]. This reactive enzyme finally catalyzed BaP degradation through hydroxylation.

3.3. Exometabolomics and phospholipid mechanisms of benzo(a)pyrene degradation

Exometabolites generate via diffusion through broken membranes or active transport. Several flux into extracellular solution as a result of membrane collapse. In the present study, the fact that only malonate, 3-phosphoglycerate, citrate, N-acetyl-D-mannosamine, ribose-5-phosphate, glucose-6-phosphate and trehalose of high concentrations were found in the solution shows that they were upsynthesized and actively released by cells during BaP degradation (Fig. 3). As carbon substrates, glucose, pyridoxine and thioctic acid were used up in this situation. These findings show that metabolic pathways of glycolysis, the pentose phosphate pathway, amino sugar and nucleotide sugar metabolism were upregulated after BaP degradation.

Both the increased use of extracellular glucose and glucose-1-phosphate and the enhanced release of glucose-6-phosphate serve as direct evidence that glycolysis was enhanced during BaP degradation. Glucose-6-phosphate dehydrogenase with an 85% increase in enzyme activity resulted in the upgeneration of glucose-6-phosphate [30]. In the pathway of fructose and mannose metabolism, mannitol was uptransformed through successive catalysis by mannitol 1-phosphotransferase and mannitol-1-phosphate 5-dehydrogenase with the production of fructose-6-phosphate. This product was further used for upregulated glycolysis in the presence of BaP. Our comparative proteomic analysis shows that many differential proteins in *Microbacterium* sp. cells are involved in glucose, benzene ring, citrate cycling, amino acid, and lipid metabolism after BaP degradation [31]. These metabolic proteins catalyzed chemical reactions similar to those observed in our recent metabolism studies.

In the pathway of amino sugar and nucleotide sugar metabolism, the enhanced transformation of UDP-*N*-acetyl-alpha-D-glucosamine produced more N-acetyl-D-mannosamine and uridine diphosphate (UDP). Before glucose was transformed into glycogen, enzyme UDP-glucose pyrophosphorylase catalyzed a UDP-glucose unit by combining a glucose-1-phosphate with a uridine triphosphate. Then, the enzyme

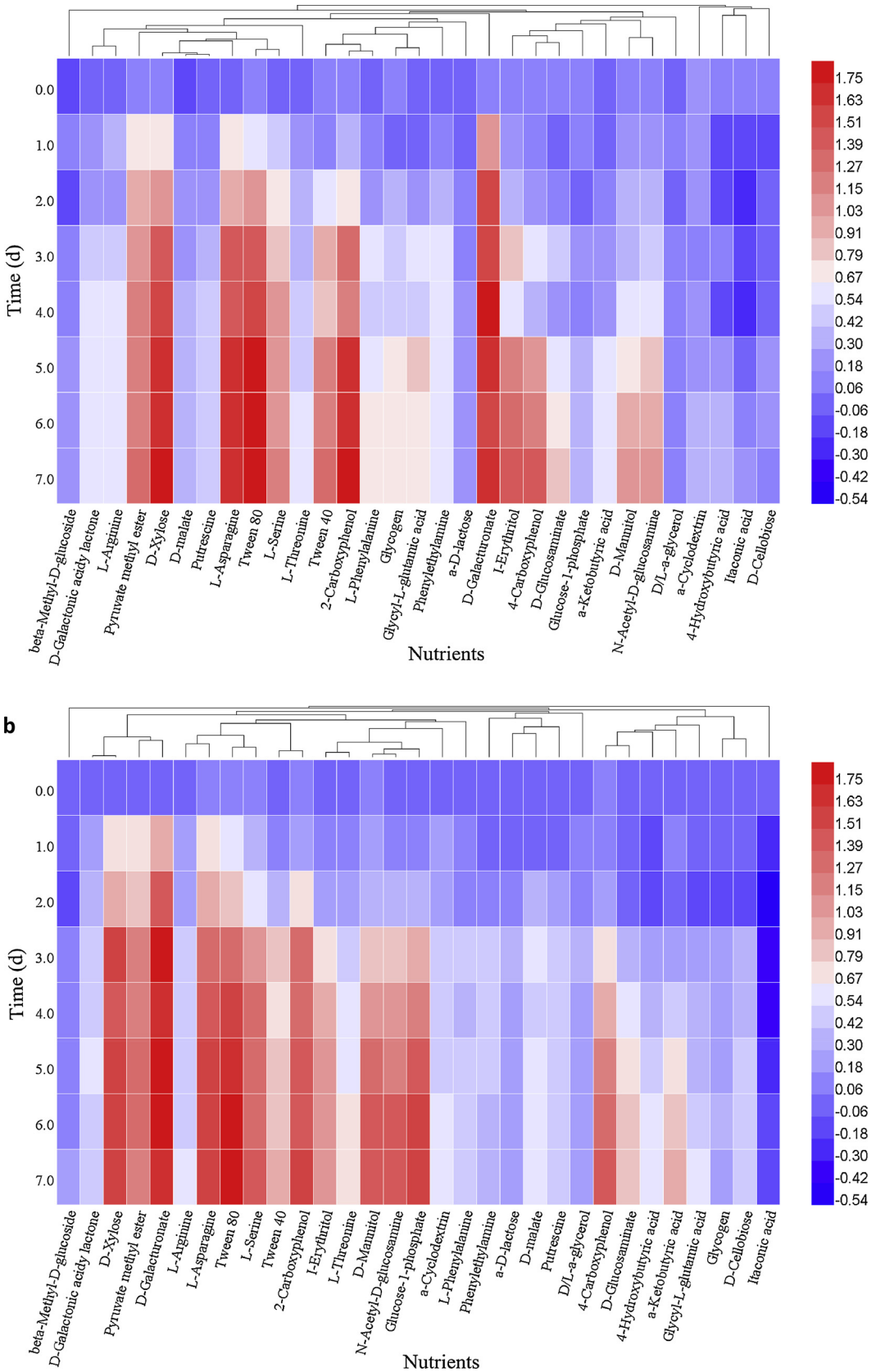

Fig. 4. Metabolism of extracellular carbon substrates. (a) The control cells before BaP degradation; (b) The treated cells after BaP degradation.

glycogen synthase combined UDP-glucose units to form a glycogen chain. The increased release of N-acetyl-D-mannosamine resulted in a decline in glycogen production. This finding is consistent with the decline of glycogen metabolism observed during BaP degradation (Fig. 3).

The concentrations of all detected phospholipids, including

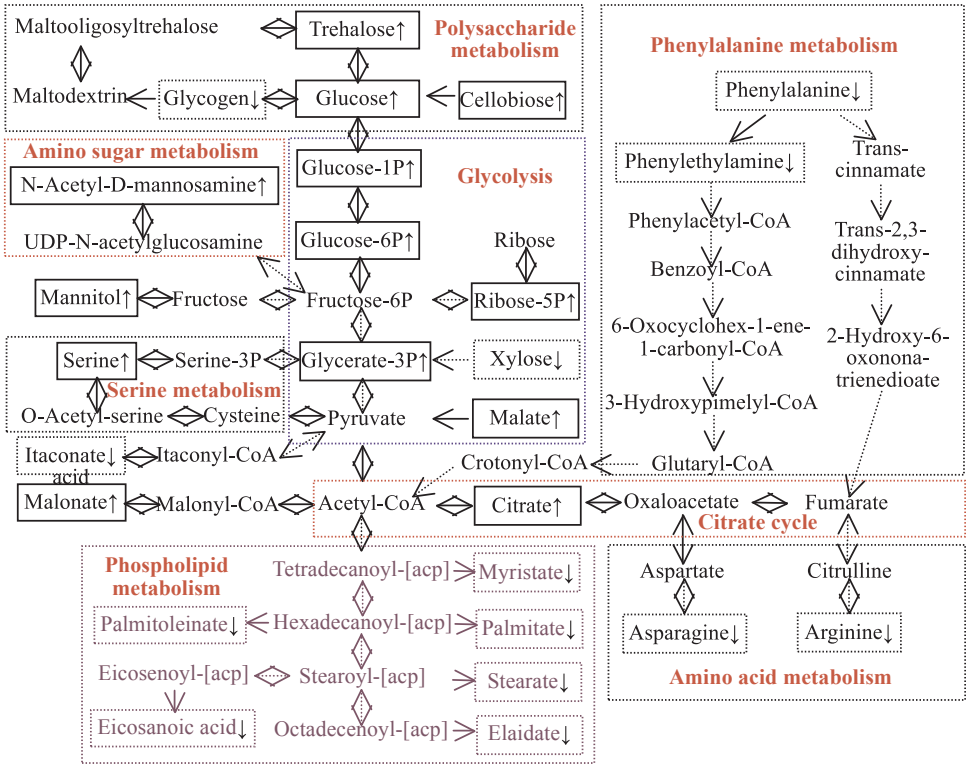

Fig. 5. Differential regulated network of cellular metabolism for BaP degradation.

myristate, pentadecanoic acid, palmitoleinate, 11-hexadecenoic acid, palmitate, cis-10-heptadecanoic acid, heptadecanoic acid, elaidate, stearate, cis-10-nonadecanoic acid and cis-11-eicosenoic acid, were downsynthesized after BaP degradation. This finding shows that precursors of phospholipid biosynthesis were transformed to intermediates used in other pathways. Malonate produced in the pathway of fatty acid metabolism served as one of these intermediates with enhanced release patterns.

3.4. Metabolism of carbon substrates after benzo(a)pyrene degradation

Substrates pyruvate methyl ester, xylose, galacturonate, asparagine, serine, tween 40, tween 80,2-carboxyphenol, 4-carboxyphenol, mannitol, erythritol and N-acetyl-D-glucosamine were easily used by the control cells before BaP degradation while β-methyl-D-glucoside, α-cyclodextrin, 4-hydroxybutyric acid, cellobiose, glucose-1-phosphate, α-lactose, glycerol and malate were difficult to metabolize (Fig. 4a and Table S3a). Overtime, the upmetabolism of compounds with benzene rings including 2-carboxyphenol, 4-carboxyphenol, phenylalanine and phenylethylamine shows that *B. thuringiensis* can degrade polycyclic aromatic hydrocarbon. As compounds with a benzyl group, they were metabolized through the benzoate degradation pathway [6,10].

In this pathway, 2-carboxyphenol and 4-carboxyphenol were sequentially catalyzed with the production of dihydroxybenzoate, hydroxyquinol, 1,2-benzenediol, cis, cis-muconate, 3-oxoadipate, ethanol and pyruvate. Regarding molecular structures, 2-carboxyphenol and 4-carboxyphenol are compounds with hydroxy and carboxyl groups attached to a benzene ring while phenylalanine and phenylethylamine have only a connected group. This is why the metabolism of 2-carboxyphenol and 4-carboxyphenol was more active than the metabolism of the other two. These results confirm that the insertion of one atom of oxygen into the benzene ring was central to ring cleavage. P450 enzymes include monooxygenase, which catalyzes the transfer of one atom of molecular oxygen to a substrate [32]. Our carbon metabolism results are consistent with this function of P450.

After BaP degradation, the metabolism of serine, mannitol, N-acetyl-D-glucosamine, cellobiose, glucose-1-phosphate, glycerol and malate was significantly upregulated while the use of arginine, asparagine, phenylalanine, phenylethylamine, xylose, glycogen and itaconic acid was significantly downregulated (Fig. 4b and Table S3b). In the benzoate degradation pathway, reactions of oxygenation catalyzed by oxidoreductase and hydrolase were required for benzene ring cleavage. Enzymes involved in this process were also responsible for BaP transformation. For example, BaP mediated aryl hydrocarbon receptors in lung cells are required for the stimulation of mitogen activated protein kinase signaling cascade [11] and for the transformation of aryl compounds. This is why the metabolism of phenylalanine and phenylethylamine was downregulated in the presence of BaP.

For amino acids metabolism, serine was catalyzed by phosphoserine phosphatase and cysteine synthase, resulting in the generation of cysteine (Fig. 5). The upmetabolism of serine observed in the current work is consistent with the upsynthesis of cysteine in human bladder cancer cell line RT4 [29] and in *S. maltophilia* under BaP exposure [16], inducing a metabolic shift from glycolysis to the pentose phosphate pathway triggered by BaP. These results show that key antioxidant molecule glutathione stemmed from the transformation of cysteine was upsynthesized through the detoxification of reactive oxygen species, the level of which was enhanced under BaP stress.

Asparagine was transformed into aspartate, which was further degraded by aminotransferase. The produced oxaloacetate generated various intermediates in several metabolic processes. Amino acid arginine was also transformed into argininosuccinate in the presence of fumarate and argininosuccinate lyase. Argininosuccinate was catalyzed by argininosuccinate synthase, generating aspartate, a precursor of the citrate cycle. Therefore, both asparagine and arginine were catalyzed through the same pathway after being transformed into aspartate. Thus, the transformation of asparagine and arginine into aspartate was inhibited by BaP. These results are supported by the interrupted metabolism of asparagine in the rat cerebellum under BaP stress [33]. Although the synthesis of arginine in *Pinctada martensii* underwent an

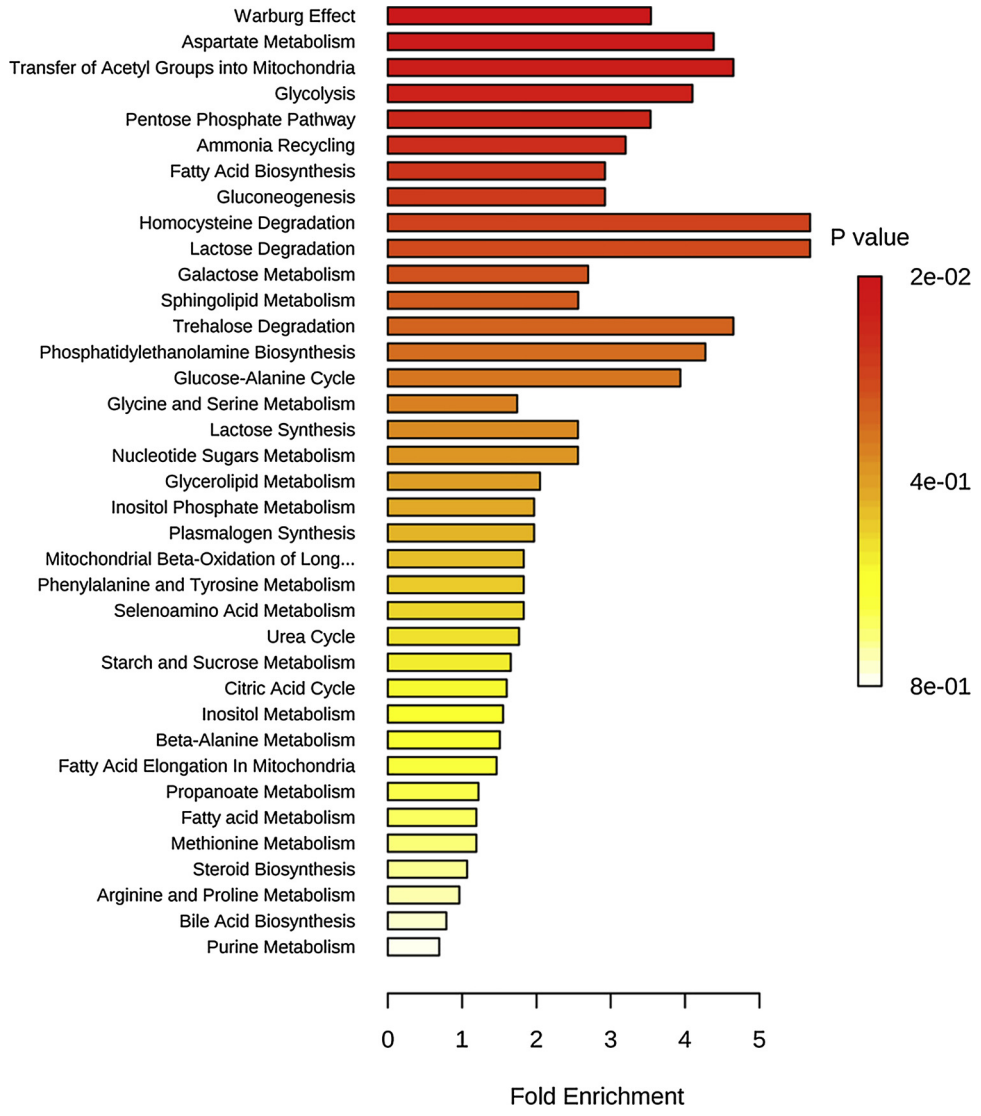

Fig. 6. The impact of BaP degradation on cellular metabolism pathways.

upregulated trend [34], the arginine metabolism pathway was found to be one of the target pathways significantly altered by BaP.

Glycogen is a branched biopolymer consisting of linear chains of glucose residues linked linearly with α (1→4) glycosidic bonds. Branches of glycogen are linked to the chains from which they are branch from by α (1→6) glycosidic bonds. During metabolism, glycogen can be catalyzed by glucan 1,4-alpha-glucosidase via glucose production or degraded by isoamylase, maltodextrin alpha-D-glucosyltransferase and maltooligosyltrehalose trehalohydrolase to form trehalose. The disappearance of extracellular glucose and the increased release of trehalose observed on the seventh day confirm that glucose was consumed through pathways of glycolysis and polysaccharide synthesis.

During glycolysis, glucose was converted into pyruvate. In another pathway, trehalose formed from 1,1-glucoside bonds between glucose units. This finding is consistent with the upsynthesis of S-layer glycoprotein during BaP degradation by *Stenotrophomonas maltophilia* [16]. Its upsynthesis confirms that glycosylation was upregulated and glycogen metabolism was downregulated during BaP degradation. A metabolomic analysis also reveals changes in levels of glycogen and glucose observed in the hepatopancreas of male green mussels, inferring that BaP exposure affected energy metabolism [35].

Cellobiose is a disaccharide with two glucose units linked with a β(1→4) bond. It was uphydrolyzed by cellobiose glucohydrolase during BaP degradation. These findings confirm that enzymes for the cleavage of β(1→4) bonds were upsynthesized while 1,4-alpha-D-glucan glucohydrolase and 6-alpha-D-glucanohydrolase for the breakage of α-glycosidic bonds were downexpressed. After its transformation to xylulose, xylose was successively metabolized through the pentose phosphate pathway, through the glycolysis of core modules involving three-carbon compounds, and through pyruvate oxidation and citrate cycling. These successive pathways and itaconate metabolism via C5-branched dibasic acid metabolism were depressed by BaP and its intermediates.

3.5. Pathway enrichment related to benzo(a)pyrene degradation

To quantitatively clarify the impact of BaP degradation on cellular metabolism pathways, the pathway enrichment of the metabolic data was analyzed through the metaboanalyst database (http://www.metaboanalyst.ca/). Fig. 6 shows that the degradation process was significantly correlated with cysteine, lactose and trehalose degradation, aspartate metabolism, phosphatidylethanolamine, sphingolipid, glycerolipid and fatty acid biosynthesis, and the transfer of acetyl groups into membrane and pentose phosphate pathways. Phosphatidylethanolamine, sphingolipid and glycerolipid are three different families of phospholipids. Acetyl groups are commonly transferred from

acetyl-CoA to coenzyme A. Acetyl-CoA converted into malonyl-CoA by catalysis of acetyl-CoA carboxylase initiates the synthesis of fatty acids [36]. Proteins involved in acetyl group transfer in membranes are responsible for providing such groups. These results show that phospholipid metabolism is a major target pathway associated with BaP degradation because phospholipid compositions are central to the production of BaP metabolites [37]. The decreased expression of sphingolipid and free fatty acids in an alveolar type II cell line induced by 4 μM of BaP at 6 h also shows that lipid metabolism serves as a target pathway [38].

4. Conclusions

Bacillus thuringiensis can effectively metabolize compounds with benzene rings, including BaP, 2-carboxyphenol, 4-carboxyphenol, phenylalanine and phenylethylamine. During BaP degradation, phospholipid synthesis, polysaccharide degradation, asparagine, arginine, itaconate and xylose metabolism were downregulated while glycolysis, the pentose phosphate pathway, citrate cycling, amino sugar and nucleotide sugar metabolism were upregulated. Phospholipid metabolism was found to be the main target pathway associated with BaP degradation.

Acknowledgements

The authors would like to thank the National Natural Science Foundation of China (Nos. 21577049, 41501352) and the Science and Technology Project of Guangzhou City (No. 201707010255) for their financial support.

Appendix A. Supplementary data

Supplementary material related to this article can be found, in the online version, at doi:https://doi.org/10.1016/j.jhazmat.2018.12.004.

References

[1] C.Y. Cai, S.Y. Yu, X.Y. Li, Y. Liu, S. Tao, W.X. Liu, Emission characteristics of polycyclic aromatic hydrocarbons from pyrolytic processing during dismantling of electronic wastes, J. Hazard. Mater. 351 (2018) 270–276.
[2] A.K. Sivaram, P. Logeshwaran, R. Lockington, R. Naidu, M. Megharaj, Impact of plant photosystems in the remediation of benzo[a]pyrene and pyrene spiked soils, Chemosphere 193 (2018) 625–634.
[3] Z.S. Yan, Y.H. He, H.Y. Cai, J.D. van Nostrand, Z.L. He, J.Z. Zhou, L.R. Krumholz, H.L. Jiang, Interconnection of key microbial functional genes for enhanced benzo[a] pyrene biodegradation in sediments by microbial electrochemistry, Environ. Sci. Technol. 51 (2017) 8519–8529.
[4] M. Cecotti, B.M. Coppotelli, V.C. Mora, M. Viera, I.S. Morelli, Efficiency of surfactant-enhanced bioremediation of aged polycyclic aromatic hydrocarbon-contaminated soil: link with bioavailability and the dynamics of the bacterial community, Sci. Total Environ. 634 (2018) 224–234.
[5] X.Y. Ma, Q.Y. Li, X.C. Wang, Y.K. Wang, D.H. Wang, H.H. Ngo, Micropollutants removal and health risk reduction in a water reclamation and ecological reuse system, Water Res. 138 (2018) 272–281.
[6] J. Stadnicka-Michalak, F.T. Weiss, M. Fischer, K. Tanneberger, K. Schirmer, Biotransformation of benzo[a]pyrene by three rainbow trout (*Onchorhynchus mykiss*) cell lines and extrapolation to derive a fish bioconcentration factor, Environ. Sci. Technol. 52 (2018) 3091–3100.
[7] S. Sushkova, I. Deryabkina, E. Antonenko, R. Kizilkaya, V. Rajput, G. Vasilyeva, Benzo[a] pyrene degradation and bioaccumulation in soil-plant system under artificial contamination, Sci. Total Environ. 633 (2018) 1386–1391.
[8] R.O. Kim, B.M. Kim, C.B. Jeong, D.R. Nelson, J.S. Lee, J.S. Rhee, Expression pattern of entire cytochrome P450 genes and response of defensomes in the benzo[a]pyrene-exposed monogonont rotifer *Brachionus koreanus*, Environ. Sci. Technol. 47 (2013) 13804–13812.
[9] T. Hadibarata, R.A. Kristanti, Fate and cometabolic degradation of benzo[a]pyrene by white-rot fungus *Armillaria* sp. F022, Bioresour. Technol. Rep. 107 (2012) 314–318.
[10] L. Reed, I. Mrizova, F. Barta, R. Indra, M. Moserova, K. Kopka, H.H. Schmeiser, C.R. Wolf, C.J. Henderson, M. Stiborova, D.H. Phillips, V.M. Arlt, Cytochrome b5 impacts on cytochrome P450-mediated metabolism of benzo[a]pyrene and its DNA adduct formation: studies in hepatic cytochrome b5/P450 reductase null (HBRN) mice, Arch. Toxicol. 92 (2018) 1625–1638.
[11] G. Vázquez-Gómez, L. Rocha-Zavaleta, M. Rodríguez-Sosa, P. Petrosyan, J. Rubio-Lightbourn, Benzo[a]pyrene activates an AhR/Src/ERK axis that contributes to CYP1A1 induction and stable DNA adducts formation in lung cells, Toxicol. Lett. 289 (2018) 54–62.
[12] Z.W. Chang, M. Lu, K.J. Shon, J.S. Park, Functional expression of *Carassius auratus* cytochrome P4501A in a novel *Shewanella oneidensis* expression system and application for the degradation of benzo[a]pyrene, J. Biotechnol. 179 (2014) 1–7.
[13] L.H. Zhang, X.C. Duan, N.N. He, X. Chen, J.L. Shi, W.M. Li, L. Xu, H.X. Li, Exposure to lethal levels of benzo[a]pyrene or cadmium trigger distinct protein expression patterns in earthworms (*Eisenia fetida*), Sci. Total Environ. 595 (2017) 733–742.
[14] A.M. Krais, E.N. Speksnijder, J.P.M. Melis, R. Indra, M. Moserova, R.W. Godschalk, F.J. van Schooten, A. Seidel, K. Kopka, H.H. Schmeiser, M. Stiborova, D.H. Phillips, M. Luijten, V.M. Arlt, The impact of p53 on DNA damage and metabolic activation of the environmental carcinogen benzo[a]pyrene: effects in *Trp53*(+/+), *Trp53*(+/-) and *Trp53*(-/-) mice, Arch. Toxicol. 90 (2016) 839–851.
[15] Q. Shi, R.W.L. Godschalk, F.J. van Schooten, Inflammation and the chemical carcinogen benzo[a]pyrene: partners in crime, Mutat. Res-Rev. Mutat. 774 (2017) 12–24.
[16] S.N. Chen, H. Yin, J.J. Chang, H. Peng, Z. Dang, Physiology and bioprocess of single cell of *Stenotrophomonas maltophilia* in bioremediation of co-existed benzo[a]pyrene and copper, J. Hazard. Mater. 321 (2017) 9–17.
[17] Z.Y. Li, Y.H. Wu, Y.Y. Huo, H. Cheng, C.S. Wang, X.W. Xu, Complete genome sequence of a benzo[a]pyrene-degrading bacterium *Altererythrobacter epoxidivorans* CGMCC 1.7731T, Mar. Genom. 25 (2016) 39–41.
[18] L.L. Wang, J.S. Ye, H.S. Ou, H.M. Qin, Y. Long, J. Ke, Triphenyltin recognition by primary structures of effector proteins and the protein network of *Bacillus thuringiensis* during the triphenyltin degradation process, Sci. Rep. 7 (2017) 4133.
[19] K. Mandal, B. Singh, M. Jariyal, V.K. Gupta, Microbial degradation of fipronil by *Bacillus thuringiensis*, Ecotox. Environ. Safe. 93 (2013) 87–92.
[20] M.A. Surhio, F.N. Talpur, S.M. Nizamani, F. Amin, C.W. Bong, C.W. Lee, M.A. Ashraf, M.R. Shah, Complete degradation of dimethyl phthalate by biochemical cooperation of the *Bacillus thuringiensis* strain isolated from cotton field soil, RSC Adv. 4 (2014) 55960–55966.
[21] S.N. Chen, H. Yin, J.S. Ye, H. Peng, N. Zhang, B.Y. He, Effect of copper(II) on biodegradation of benzo[a]pyrene by *Stenotrophomonas maltophilia*, Chemosphere 90 (2013) 1811–1820.
[22] A. Lubbe, B.P. Bowen, T. Northen, Exometabolomic analysis of cross-feeding metabolites, Metabolites 7 (2017) 50, https://doi.org/10.3390/metabo7040050.
[23] M.P.G. de Llasera, J. de J. Olmos-Espejel, G. Díaz-Flores, A. Montaño-Montiel, Biodegradation of benzo(a)pyrene by two freshwater microalgae *Selenastrum capricornutum* and *Scenedesmus acutus*: a comparative study useful for bioremediation, Environ. Sci. Pollut. Res. 23 (2016) 3365–3375.
[24] L.T. Tang, L.L. Wang, H.S. Ou, Q.S. Li, J.S. Ye, H. Yin, Correlation among phenyltins molecular properties, degradation and cellular influences on *Bacillus thuringiensis* in the presence of biosurfactant, Biochem. Eng. J. 105 (2016) 71–79.
[25] L.T. Serebryakova, N.A. Zorin, A.A. Karyakin, Improvement of hydrogenase enzyme activity by water-miscible organic solvents, Enzyme Microb. Technol. 44 (2009) 329–333.
[26] M. Yang, H.M. Qin, W.H. Wang, H.L. Zhang, Y. Long, J.S. Ye, Global proteomic responses of *Escherichia coli* and evolution of biomarkers under tetracycline stress at acid and alkaline conditions, Sci. Total Environ. 627 (2018) 1315–1326.
[27] W.Y. Yi, K.L. Yang, J.S. Ye, Y. Long, J. Ke, H.S. Ou, Triphenyltin degradation and proteomic response by an engineered Escherichia coli expressing cytochrome P450 enzyme, Ecotox. Environ. Safe. 137 (2017) 29–34.
[28] K.H. Kim, C.W. Lee, B. Dangi, S.H. Park, H. Park, T.J. Oh, J.H. Lee, Crystal structure and functional characterization of a cytochrome P450 (BaCYP106A2) from *Bacillus* sp. PAMC 23377, J. Microbiol. Biotechnol. 27 (2017) 1472–1482.
[29] F.P. Guengerich, A.W. Munro, Unusual cytochrome P450 enzymes and reactions, J. Biol. Chem. 288 (2013) 17065–17073.
[30] N. Verma, M. Pink, S. Boland, A.W. Rettenmeier, S. Schmitz-Spanke, Benzo[a]pyrene-induced metabolic shift from glycolysis to pentose phosphate pathway in the human bladder cancer cell line RT4, Sci. Rep. 7 (2017) 9773.
[31] W. Qin, F.Q. Fan, Y. Zhu, Y.Y. Wang, X. Liu, A.Z. Ding, J.F. Dou, Comparative proteomic analysis and characterization of benzo(a)pyrene removal by *Microbacterium* sp. strain M.CSW3 under denitrifying conditions, Bioproc. Biosyst. Eng 40 (2017) 1825–1838.
[32] Z.W. Yan, Z.B. He, Z.T. Yan, F.L. Si, Y. Zhou, B. Chen, Genome-wide and expression-profiling analyses suggest the main cytochrome P450 genes related to pyrethroid resistance in the malaria vector, Anopheles sinensis (*Diptera Culicidae*), Pest Manag. Sci. 74 (2018) 1810–1820.
[33] C.L. Li, J. Wang, Q.P. Su, K. Yang, C.Z. Chen, X.J. Jiang, T.L. Han, S.Q. Cheng, T.T. Mo, R.Y. Zhang, B. Peng, Y.M. Guo, P.N. Baker, B.J. Tu, Y.Y. Xia, Postnatal subacute benzo(a) pyrene exposure caused neurobehavioral impairment and metabolomic changes of cerebellum in the early adulthood period of sprague-dawley rats, Neurotox. Res. 33 (2018) 812–823.
[34] H. Chen, X.P. Diao, H.H. Wang, H.L. Zhou, An integrated metabolomic and proteomic study of toxic effects of Benzo[a]pyrene on gills of the pearl oyster Pinctada martensii, Ecotox. Environ. Safe. 156 (2018) 330–336.
[35] Q.Q. Song, H.L. Zhou, Q. Han, X.P. Diao, Toxic responses of *Perna viridis* hepatopancreas exposed to DDT, benzo(a)pyrene and their mixture uncovered by iTRAQ-based proteomics and NMR-based metabolomics, Aquat. Toxicol. 192 (2017) 48–57.
[36] M.F. Renne, A.I.P.M. de Kroon, The role of phospholipid molecular species in determining the physical properties of yeast membranes, FEBS Lett. 592 (2018) 1330–1345.
[37] M. Stiborova, R. Indra, M. Moserova, L. Bor˘ek-Dohalska, P. Hodek, E. Frei, K. Kopka, H.H. Schmeiser, V.M. Arlt, Comparison of human cytochrome P450 1A1-catalysed oxidation of benzo[a]pyrene in prokaryotic and eukaryotic expression systems, Monatsh. Chem. 148 (2017) 1959–1969.
[38] S.Y. Zhang, D.Q. Shao, H.Y. Liu, J. Feng, B.H. Feng, X.M. Song, Q. Zhao, M. Chu, C.T. Jiang, W. Huang, X. Wang, Metabolomics analysis reveals that benzo[a]pyrene, a component of PM2.5, promotes pulmonary injury by modifying lipid metabolism in a phospholipase A2-dependent manner in vivo and in vitro, Redox Biol. 13 (2017) 459–469.